Viruses as a tool in nanotechnology and target for conjugated polymers

Gruszka, Agnieszka

Chapter 2 Single Walled Carbon Nanotubes as template for formation of Virus-Like Particles

2.1 Introduction

Conjugation of biomolecules with synthetic materials is a rapidly expanding field and it holds great promise for future applications in miniaturized electronics and tissue engineering. In this chapter, hybrids made of proteins and carbon nanotubes (CNTs) are in the focus. These two components exhibit very different characteristics. Carbon nanotubes are one dimensional objects built of graphene sheets rolled up in a seamless cylinder. This nanostructure is therefore rigid, mechanically and chemically stable and exhibits conducting or semiconducting properties. However, CNTs in their pristine form are not compatible with biological systems because they lack solubility in aqueous medium. Proteins, on the other hand, consist of polypeptide chains, which fold into nanometer-sized, three dimensional structures that are responsible for many biological functions. When compared to CNTs, they are rather sensitive and instable in extracellular environment. Thus, combination of the advantages of these two worlds can offer unprecedented performance when complementing each other regarding their physical, chemical and biological properties.

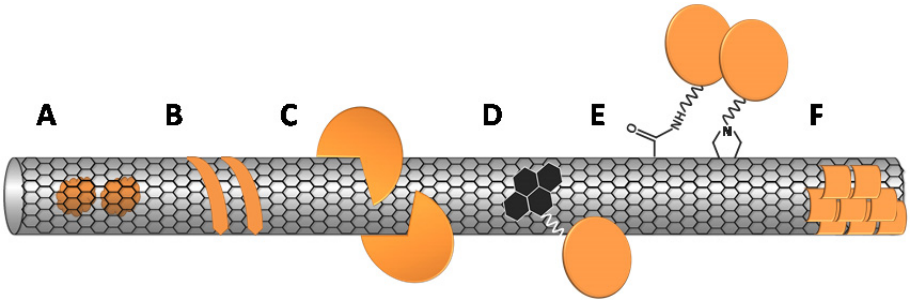

Figure 2.1. Interactions of proteins with carbon nanotubes. Proteins can be accommodated in the hollow interior of a nanotube (A) or adsorbed on the surface (B-F); Short peptides can be designed to tightly wrap the CNTs (B), whereas larger native proteins mainly interact via hydrophobic domains (C); Adsorption can be also achieved by introducing a linker exhibiting affinity to the surface (D); Covalent binding of proteins to the surface of CNT's can be achieved via activated carboxylic groups, introduced on the CNT surface through oxidation, or via cycloaddition reactions (E); In rare occasions hierarchical organization of proteins on the surface of CNTs is also possible (F).

To exploit the properties of both materials, the two components need to be successfully coupled. The hollow nature of CNTs was quickly recognized as an opportunity for new loading strategies (Figure 2.1A). Entry of proteins into the carbon nanotube has been demonstrated with small globular enzymes[1]. However, the interior of the CNT was identified as destabilizing because the accommodated proteins tend to interact with the hydrophobic inner surface of the CNTs. As a consequence, proteins gradually undergo conformational changes and thereby lose their functionality[2]. Although computational studies revealed that encapsulation of a similar protein in CNTs having the right diameter is likely to occur, this concept still remains extremely challenging to realize[3].

The outer surface of a CNT is more reachable and easier to investigate. Nonetheless, up to now very little is known about spatial distribution, structure or functioning of proteins that bind in a non-covalent fashion to the surface of the CNTs (Figure 2.1B and 2.1C)[4]. In general, protein adsorption is governed by four types of interactions: π-π stacking, hydrophobic interactions, van der Waals forces and electrostatic interactions. Furthermore, it has been concluded that amphiphilicity is the key factor ensuring formation of CNT-protein hybrids in aqueous media[5]. The composition of the polypeptide chain is not determinant of the binding to a CNT, as long as hydrophobic and solubility-ensuring hydrophilic domains coexist within the secondary and tertiary

structure[4]. Additionally, the hydrophobic domains must be able to accommodate the carbon nanotube in a natural cavity or upon conformational changes. Obviously, short synthetic peptides may exhibit similar properties. In fact, CNT dispersing sequences have been identified via computational calculations and the phage-display technique[6]. Even chiral sorting of Single Walled CNTs (SWCNTs) has been achieved with a variety of peptides, including cyclic ones with tailored diameters[4]. In all cases achieving a stable dispersion of unbundled CNTs is a critical step and the starting point for any application.

For formation of functional materials, CNTs can also serve as a platform for enzyme immobilisation[7,8]. The binding strategy needs to be carefully designed. Just as with other immobilization resins, proteins can lose most of their activity upon binding[8]. To deal with this issue, a linker molecule between the CNT and protein was suggested (Figure 2.1D and 2.1E). The linker itself has to be long and flexible enough to allow the protein to maintain the right conformation. Moreover it should allow for orthogonal protein coupling strategies. The biological entity can be attached to the CNTs in a covalent or non-covalent fashion[3]. The non-covalent binding requires presence of a polyaromatic unit such as pyrene, which is responsible for docking onto the CNT's surface (Figure 2.1D). This strategy is often preferred as it doesn't affect the structure of the CNT walls. The covalent binding mostly involves amino–linkers that react with activated carboxyl groups formed on the oxidized tube surface or diazo compounds that undergo a cycloaddition reaction (Figure 2.1E). Unfortunately, in both approaches the unspecific binding of proteins to the CNT's wall cannot be excluded. Such unwanted interactions often lead to the presence of partially unfolded biologicals, which impairs the function of both the CNT and protein[3,9].

Despite all difficulties, such combination of materials has been widely explored. For example, the mechanical properties and geometry of the CNTs have stimulated their application as bioscaffolds to reinforce tissues. CNTs functionalized with specific peptides or extracellular matrix proteins like fibronectin or collagen can support cell adhesion, growth and even differentiation[10]. Additionally, these materials offer new properties due to the electrical conductivity of the tubes, which is particularly interesting when combined with conductive tissues such as cardiac cells or neurones. It has been demonstrated that laminin coated nanotubes are a suitable substrate for neuronal adhesion as they

promote neurite elongation[11]. Finally, the possibility of incorporation of contrast agents in the intratubular space of the CNTs potentially enables monitoring of tissue growth on CNT-scafffolds. Such loading has been achieved with a variety of materials interesting for medical diagnostics like Fe_2O_3 or Gd^{3+} ions, that are also used for magnetic resonance imaging, I_2 used for X-ray computed tomography and even radionuclides were incorporated and employed for emission tomography or radiotherapy[4].

Ever since it was demonstrated that carbon nanotubes can be internalized by living cells their hybrids rapidly gained attention. CNTs have been employed as a drug delivery system for anti-cancer drugs, antibiotics, proteins and even nucleic acids intended for gene therapy[4]. The cell entry is not specific though and the exact mechanism is still under debate as endocytosis seems to be as likely as a direct piercing of the cellular membrane[12]. Despite ambiguity of this process, there are several prominent examples of utilizing CNTs for medical applications. For example, tumour targeting hybrids for phototherapy were generated by coating CNTs with antibodies which attach to lymphoma cells. Thereby, the optical properties of the nanotubes were explored. Upon near infrared irradiation of the tumour, the CNTs heated up and were able to destroy nearby cancer cells selectively. Another reported application takes advantage of the unique shape of the nanotubes. The CNTs were found to interact with microtubules because of their similar geometry, which promoted interaction of both and resulted in formation of dysfunctional hybrids that led to the cell death[13]. This is a very interesting finding since many anticancer drugs target microtubule dynamics. Lastly, CNTs were used as scaffolds for multipresentation systems in vaccination research. Many short antigenic peptides are not immunogenic enough to activate specific antibodies. However, it was shown that CNTs functionalized with haptens can trigger an immunoresponse and may be valuable components of synthetic vaccines[14].

It has to be noted here that the toxicity of CNTs has emerged as a problem when research on their bioapplication significantly advanced. The toxicological profile of CNTs is complicated due to unspecific binding with many proteins. For instance, it was shown that they interact with actin structures and therefore strongly supress cell proliferation[15]. Moreover, it was speculated that SWCNTs block the pores of ion channels. In general, specific functionalization of the surface

by non-covalent protein binding or chemical functionalization is desired because that may reduce unspecific interactions with the hydrophobic surface and may lower their cytotoxicity[4,16].

Despite all the efforts spent for functionalization of CNTs, formation of a highly ordered layer of proteins wrapping the surface of the carbon nanotubes still remains a challenge (Figure 2.1F). Previously it was demonstrated that streptavidin can crystalize on Multi Walled CNTs (MWCNTs). Following this study, molecular dynamics simulation experiments revealed that such hybrids cannot be efficiently formed on CNTs with diameter smaller than 10 nm due to the high curvature. This in theory excludes the utilization of all SWCNT and also might give an explanation why most proteins preferentially bind to bundled CNTs[3].

In this chapter we aim to encapsulate SWCNTs in a uniform protein shell. Here, coat proteins of plant viruses represent excellent candidates due to their plasticity and cooperative nature. To achieve successful encapsulation of SWCNT in virus-like particle (VLPs), we designed a two step assembly method using different biological macromolecules. First, an aqueous solution of monodisperse SWCNTs was obtained with help of DNA. The resulting SWCNT dispersions were then further investigated as scaffold for assembly of plant virus capsid proteins. Three candidates were evaluated as protein shell donor: Tobacco Mosaic Virus (TMV), Potato Virus X (PVX) and Cowpea Chlorotic Mottle Virus (CCMV). The interactions of virus capsids with SWCNTs was investigated with Transmission Electron Microscopy (TEM).

2.2 Results and discussion

2.2.1 Preparation of SWCNT dispersion

To date, single stranded (ss) oligonucleotides have been widely used to disperse CNTs and to aid manipulation of the solubilized structures[17,18]. As demonstrated with molecular dynamic approaches, application of oligonucleotides as a dispersant provides a uniform layer of negative charges distributed along the CNT surface. Therefore, DNA was employed as a mediating agent in the VLP assembly process. Additionally, DNA is closely related to the natural cargo of RNA-viruses which will be included in this study, while being cheaper and more stable.

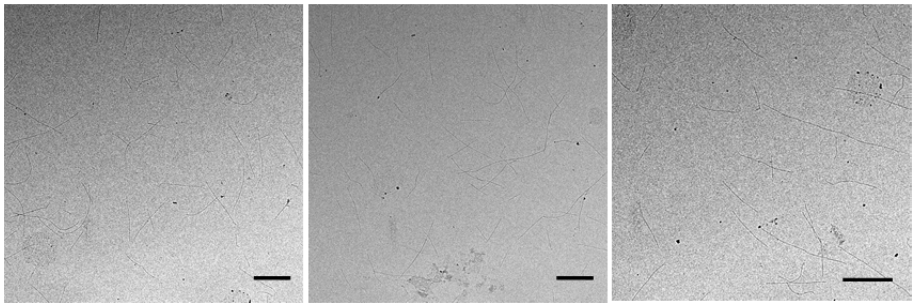

Figure 2.2. Representative TEM images of SWCNTs dispersed with a 22-mer DNA. Scale bars 500 nm.

In principle any DNA sequence is able to disperse CNTs in water[19]. Therefore, in the following experiments we employed a 22-mer sequence that lacks secondary structures and which was already utilized in VLPs templating experiments as well as in CNTs dispersions [20,21]. In order to obtain SWNTs in an aqueous environment, 1 mg/mL of DNA solution was added in portions to solid SWCNTs. Next, the mixture was placed in a cold sonication bath for the total time of 2.5 h and the mixture was afterwards centrifuged to remove insoluble carbon material. The excess DNA which didn't bind to the SWCNTs surface was removed in a centrifugal dialysis device. The efficiency of dispersion has been estimated to be 8% which corresponds to reported values (~10%)[19]. As shown in Figure 2.2, individually dispersed SWCNTs are abundant in the sample and no major bundles of CNTs are detected. The average length of the CNTs is 500-800 nm, which is comparable to the values provided by the manufacturer (<1000 nm). Due to the short and low energy sonication process, the CNTs were not significantly shortened[22]. The measured diameter of the single tubes falls in the range of 3-5 nm. This is slightly larger than the 0.8-1.2 nm reported by the manufacturer and can be attributed to the wrapping by DNA.

2.2.2 Tobacco Mosaic Virus

The first virus candidate studied as a potential building block of SWCNT-protein hybrid is Tobacco Mosaic Virus. TMV as well as SWCNT exhibit rigid, rod-like geometries. We anticipated that these structural similarities would greatly facilitate the co-assembly process with the DNA dispersed CNTs.

TMV infects exclusively plans. It is a filamentous virus formed by 2100 coat proteins (CPs) and a single RNA strand embedded deeply within the 4 nm inner channel. The wild type (WT) particle is typically 18 nm wide and 300 nm long[23]. The assembled virus represents a very robust biomaterial, being incomparably more stable and insensitive than single TMV CPs. It can withstand high temperatures up to 90°C and even the presence of organic solvents. Additionally, TMV can be uniformly deposited on surfaces or even spin-coated in topographically structured arrays. As such, TMV was widely used as a composite in hybrids with inorganic materials where the inner cavity and the outer surface are available for modification[24]. For example, it was employed to build metallic 1-D nanowires and it served as scaffold for light harvesting systems[23]. Aside from that, TMV is being used as gene vector in "bimolecular farming" to produce i.a. human growth factor or vaccines against oncogenic human papilloma virus[23].

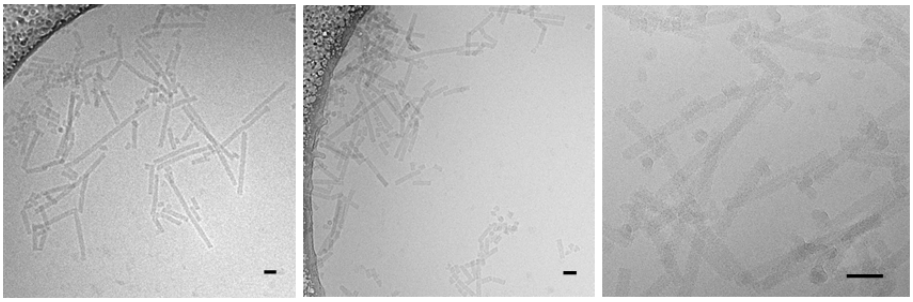

Figure 2.3. Different cryo-EM micrographs of TMV assembled at pH 5.5. Scale bar 50 nm.

The process or re-assembly of TMV CP into differently shaped viral particles depends on pH and ionic strength of the buffer and was described in detail in literature and follows similar patterns in case of WT and modified viruses[25]. TMV-like empty protein tubes are spontaneously formed in an environment with pH below 6.5, as shown in Figure 2.3. They exhibit a uniform diameter of 18 nm, however, their length varies from 50 to 300 nm. Additionally, very short protein stacks are present. In neutral pH, the formed tubes disassemble into small discs, while further increasing the pH to basic values causes disassembly of TMV and proteolysis of single CPs[25]. Although TMV in tubular form has been widely exploited in material science, very little is known about assembly of these virions on anionic templates other than viral RNA. Therefore we have investigated behaviour of TMV CP exposed to DNA-dispersed CNTs.

In a first experiment, the CP of Tobacco Mosaic Virus at concentration of 0.2 mg/mL was incubated with DNA-dispersed SWCNTs at pH=5.5. It has to be noted that in low pH TMV CP preferably exist in tubular structures. After exposure to SWCNT template, changes in TMV morphology were imaged by TEM. As shown in Figure 2.4A, the TMV particles have the tendency to stick to the surface of CNTs and form bundles of viruses aligned parallel to each other. Furthermore, the virus tubes are more likely to be found along straight stretches of CNT and any curvature of the CNT seems to be incompatible with the viral geometry. The diameter of the aggregated TMV particles, which are still distinguishable within aggregates, corresponds to the diameter of TMV in the control sample. However when looking at the close up images (Figure 2.4B) single TMV tubes appear to be slightly broadened with diameter of 23±2 nm.

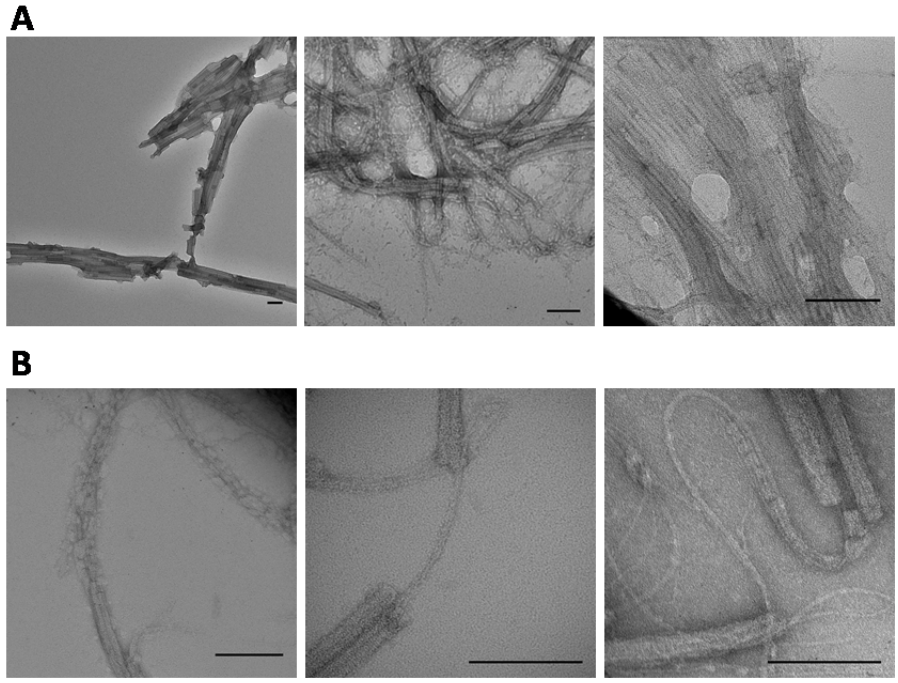

Figure 2.4. TEM micrographs of TMV CP in the presence of SWCNT dispersion. Virus protein tubes aggregate in a parallel fashion to the surface of SWCNTs (A). High magnification images reveal some degree of reassembly of the TMV CP with the surface of CNTs (B). Scale bars 100 nm.

One could argue that the observed bundles are due to coordination of the CNT to TMV's surface. The measured difference corresponds to diameter of a single SWCNT, which adheres tightly to the protein tube and therefore is hardly visible under the used negative stain conditions. Surprisingly, also rearrangement of TMV particles was observed upon exposure to SWCNT under the same conditions. To facilitate the observation of this process, the protein concentration was reduced tenfold. As it is visible in Figure 2.4B, small TMV protein assemblies (<10 nm) create a shell around the CNT. We could not detect efficient templating of individual CPs around the tubes even after prolonged incubation periods. The morphology of the formed VLPs was found to be very different from empty virus tubes. We suspect that the size of the inner cavity of TMV prevents efficient encapsulation. Secondly, the geometry of TMV hinders formation of VLPs in the curved parts of SWCNT, which therefore supresses complete coverage. Nevertheless, the presence of SWCNT in the concentrated TMV CP solution drives substantial assembly of TMV particles to form virus bundles.

2.2.3 Potato Virus X

The Potato Virus X (PVX), just as TMV, has a filamentous geometry but in contrast to the TMV virion it is more flexible. This could possibly facilitate accommodation of a SWCNT in the inner cavity and result in formation of the hybrid. The PVX particles exhibit helical symmetry and have a deeply grooved surface[26]. The WT PVX particle has a diameter of 13 nm and an average length of 500 nm[27]. The virus accommodates a single stranded RNA genome (6.4 kb) within an inner channel of 3.4 nm. One particle consist of approximately 1300 units of single CP which corresponds to 8.9 CP per turn of the virion[28].

Chimeric PVX particles expressing a variety of peptides on their surface can be efficiently produced in infected plants and evaluated and applied in research without major interference of the PVX structure. First of all, PVX is a valuable gene vector to express added-value biomolecules in plants[29,30]. Secondly, engineered PVX virions can express more than 1000 antigens per particle and therefore proved to be able to trigger a complex immune response. Such structures have been already utilized as parts of synthetic vaccines. In an in-vivo experimental set up, immunization with PVX based vaccines resulted in the formation of HIV neutralizing antibodies[31]. Moreover, engineered PVX particles have been utilized in medical diagnostics as sensors and have been employed as

scaffolds for development of bioinorganic materials for nano-electronics[32]. PVX has not been used as broadly as TMV due to difficulties in re-assembly of the isolated CP under in vitro conditions[33,34].

The PVX virions employed in this study exhibited a uniform diameter of 13 nm with an average length of around 450 nm (Figure 2.5). This is in good agreement with known values determined for WT PVX[27].

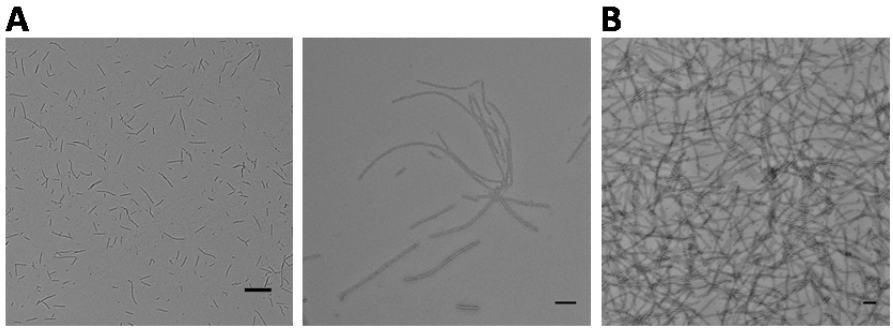

Figure 2.5. TEM micrographs of PVX virions in low (A) and high protein concentration (B). Scale bar 50 nm.

To investigate whether PVX is a suitable candidate to form protein-CNT hybrids we performed a similar experiment to the one described in the previous section. PVX particles were incubated with the SWCNT dispersion and afterwards the sample was evaluated with the help of electron microscopy. It was found that PVX undergoes substantial changes upon exposure to the SWCNTs (Figure 2.6). The observed virions were not regularly shaped and seemed to be fragmented and formation of spherical protein aggregates took place. Such aggregates are relatively large and exhibit an average size of 90 nm measured perpendicular to the CNT axis, however, they are very irregular in shape. Additionally, their attachment to the carbon nanotubes appears to be random. Strikingly, such aggregates could not be observed in the control PVX sample without SWCNTs, even at very high protein concentration (Figure 2.5B). Noteworthy is the presence of significantly shortened PVX particles (50 nm) in the same sample. This indicates that the observed protein structures are at least in part due to the PVX virion disintegration and that PVX CP favours interactions with DNA-decorated surface of the CNTs. At the same time SWCNT tubes with no signs of interactions to CPs are present in the solution. It was found that the

assembly process does not seem to be easily tuneable by variation of experimental conditions, like SWCNT to CP concentration ratio or buffer composition. The CP rearrangements were of random character and therefore the orientation of the proteins on the surface of the formed hybrids is difficult to predict. Finally, an attempt to perform the same experiment with RNA-free CP failed. Depolymerized PVX particles prepared according to previously published protocols appeared as amorphous protein and interactions with SWCNTs could not be detected[35]. This again points out the difficulty of working with PVX based VLP assemblies. It was concluded that PVX is not suitable for encapsulation of SWCNTs because the formation of such hybrid constructs needs to be robust and facile in order to make reproducible materials for future applications.

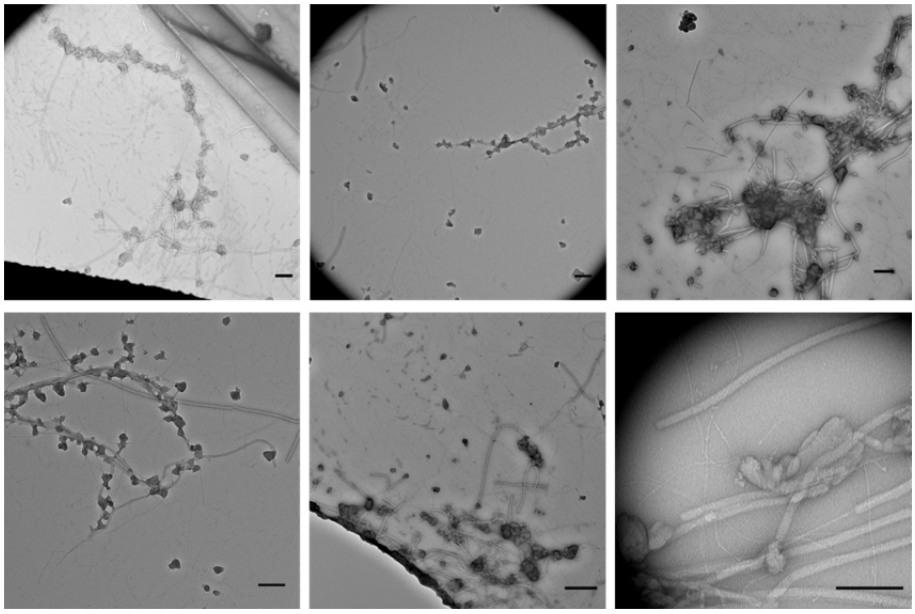

Figure 2.6. Representative TEM micrographs of PVX interaction with DNA dispearsed CNTs. Scale bar 100 nm.

2.2.4 Cowpea Chlorotic Mottle Virus

Cowpea Chlorotic Mottle Virus (CCMV) is the third plant virus candidate that was employed in this study. CCMV is an icosahedral virus composed of 180 capsid protein subunits, which encapsulate three single strands of RNA (7.9 kb in total)[36]. The outer and inner diameter of the formed

capsid are 28 and 18 nm, respectively, which corresponds to T=3 symmetry[37]. The virus can exhibit diverse geometries depending on the assembly conditions. An exceptional aspect of CCMV is the reversibility of its assembly process which was thoroughly explored. At neutral pH and high ionic strength, the virus capsid disassembles into 90 protein dimers. At this point, the viral RNA can be removed by precipitation. If the pH of CP solution drops to 5, empty capsids of the same size and geometry as the native virus re-assemble despite lack of genetic material. The empty capsids can be stored under such conditions for extended periods of time, which is advantageous for future applications. Once pH rises, the virions will disassemble again in CPs. From this point, encapsulation of any cargo in CCMV shells can proceed following either a random or template-driven way. The random method involves lowering the pH of the solution containing free CPs and a material of interest. Like described above, the virions spontaneously assemble entrapping any molecules in a statistical manner. The directed assembly approach can proceed at neutral pH, however, only in the presence of a suitable polyanionic template that mimics viral genetic material. Both possibilities were utilized to encapsulate diverse materials in CCMV VLPs as described in Chapter 1.

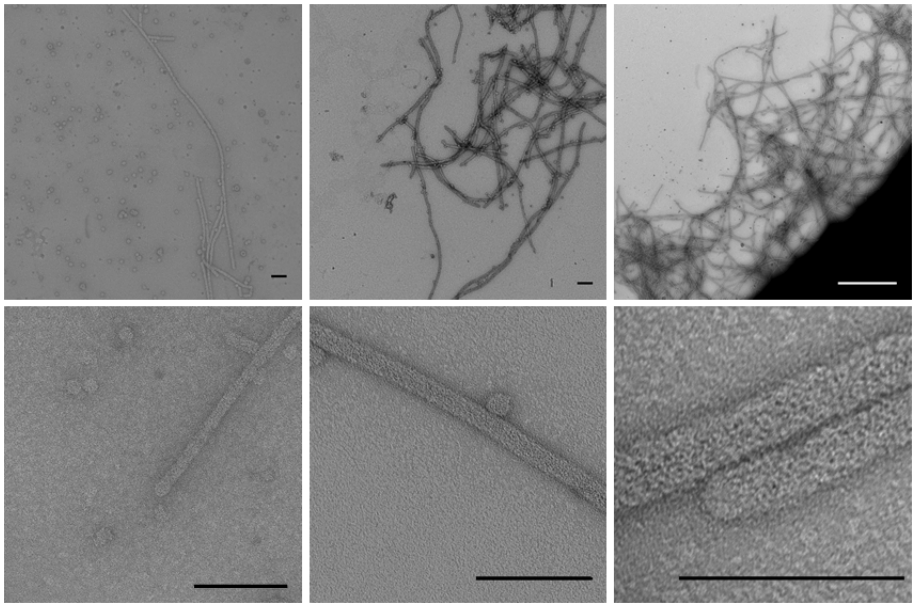

Figure 2.7. TEM micrographs of SWCNT templated CCMV assembly. Black scale bars 100 nm, white scale bar 1 µm.

To investigate the encapsulation of SWCNTs in CCMV virions, similar experiments as described above were performed. At first, the CCMV CP solution was obtained upon dialysis against a high salt buffer with pH 7.4, which causes disassembly of the empty capsids. Subsequently, the CP solution was incubated with a CNT dispersion overnight and the progress of encapsulation was evaluated by TEM. It has to be noted here that any assembly that would be observed has to be template-driven because the pH of the solution was kept neutral. As shown in Figure 2.7, efficient VLP formation took place and a protein layer was formed along the entire length of the CNTs. The resulting VLPs exhibited a uniform diameter of 22 nm, which corresponds to T=2 symmetry. Also, free CNTs were not observed in the specimen, from which one can assume that the assembly process proceeds very efficiently.

Afterwards, the same encapsulating experiment was performed with a free single stranded 22-mer. In this case, no tubular structures were observed, but instead formation of moderately uniform spherical capsids with average diameter of 26 nm ± 5nm was found (Figure 2.8). These control experiments proved that the formation of long tubular VLPs was due to the presence of the SWCNT scaffold.

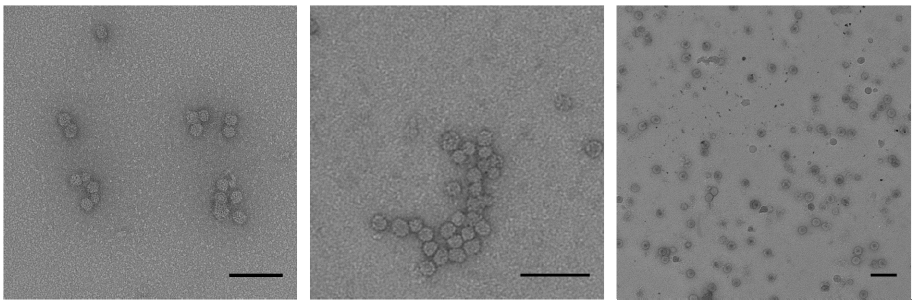

Figure 2.8. TEM micrographs of CCMV capsid formation in the presence of 22-mer DNA sequence. Scale bar 100 nm.

After proving the templated assembly, we sought confirmation of the presence of SWCNT inside the tubular protein shell and therefore cryo-EM was performed. This technique enables analysis of hybrid materials using phase contrast imaging and one can distinguish between soft protein matter and more rigid CNTs. The presence of SWCNTs inside the protein shell is shown in Figure 2.9. Remarkably, the CCMV encapsulates a single CNT regardless of its length. When closely inspecting the micrographs, half-spheres at the ends of the tube can be found, indicating that the protein shell is closed.

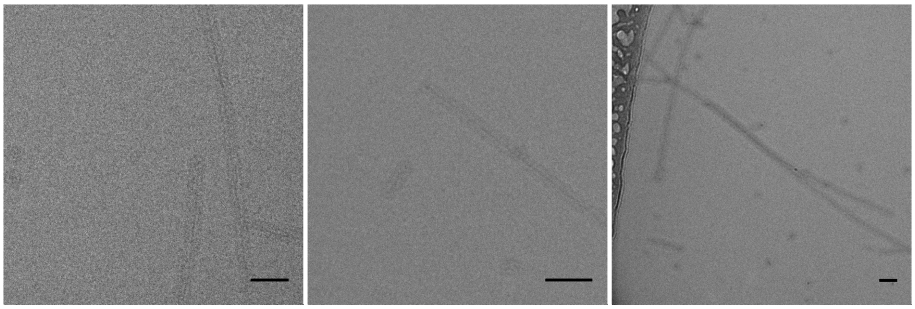

Figure 2.9. Cryo-EM images of VLP templated of SWCNT. Scale bar 50 nm.

Lastly, the mechanism of formation of the VLP was investigated. Therefore, we have monitored the progress of encapsidation of SWCNT at very early stages of incubation with CCMV CPs. As the formation of the hybrid is expected to proceed fast, the specimen was prepared almost instantly after addition of the CCMV proteins to the CNT template. As visible in Figure 2.10, the CCMV CPs appear as unstructured aggregation of capsomers attached to the surface of the CNTs at various places. This indicates that the capsid formation starts randomly at many sites on the CNT.

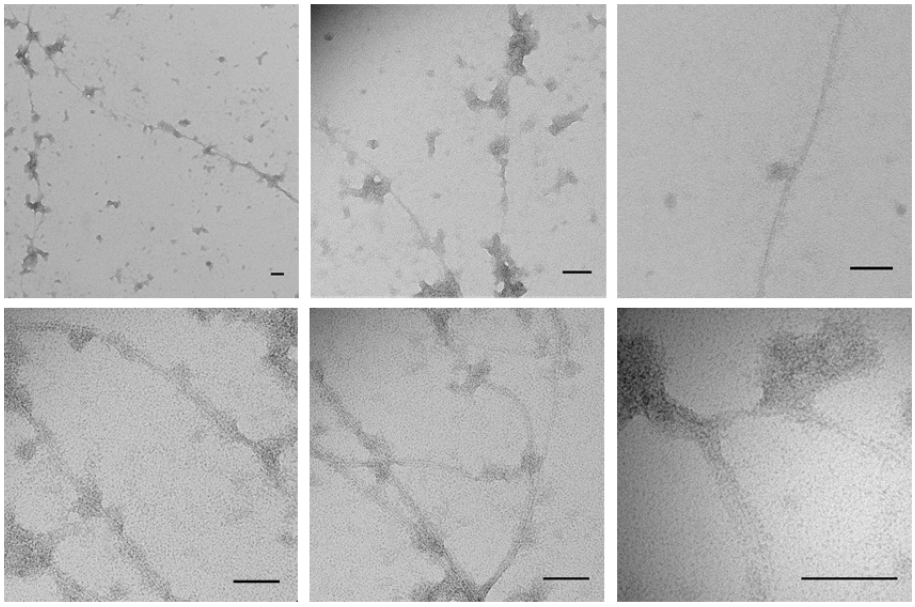

Figure 2.10. Early stage of CCMV capsids nucleation on SWCNT template. Scale bars 50 nm.

We recognized that CCMV CP in early stages of assembly follows a certain pattern which is visible on the images presented in Figure 2.11. Once viral protein recognizes the negatively charged surface of the CNT, it distributes around a CNT in a helical fashion. We assume that it is a consequence of the presence of DNA, which also wraps the CNT in a helical fashion and therefore governs the assembly pattern. Up to date the process of CCMV tube formation was not fully understood. It was suggested that the tube formation is a consequence of rolling up a protein lattice, where CP is arranged hexagonally[38]. In fact we do recognize that the CCMV protein aggregates attached to the CNT's surface exhibit a characteristic pattern that is typical for the capsomers of CCMV. However, we think that the CP gets spatially distributed. Nevertheless our results confirm that the CCMV CPs do not require specific nucleation sites for formation of the viral tubes. The virus capsid formation proceeds in a dynamic process and the CPs present in solution were able to fill up gaps after single CPs have assembled on the tubes.

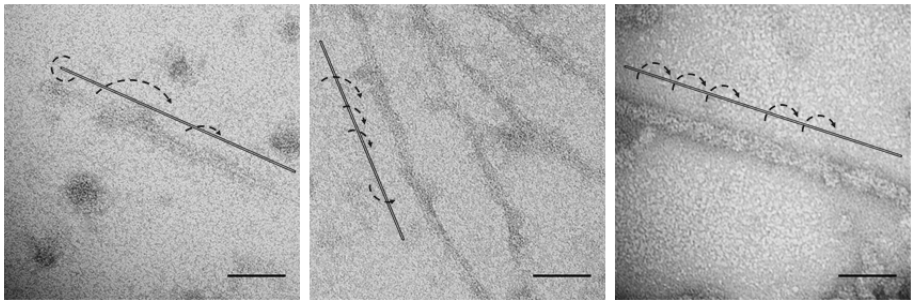

Figure 2.11. Helical assembly mode of CCMV on the DNA-dispersed SWCNT. Scale bar 50 nm.

The presented work revealed another type of synthetic material suitable for template-guided assembly of CCMV and opened new possibilities to utilize CCMV virus in applications that so far were reserved for rod-like viruses.

2.3 Conclusion

Up to date, direct interactions of proteins with the surface of CNTs have been challenging to predict and control. As a result, little is known about the fabrication of such hybrid materials. In this chapter, we demonstrated DNA-guided hybrid formation that minimizes direct contact between proteins and CNTs and yet results in a uniform protein

shell. We designed a two-step assembly process for the formation of CNT hybrids utilizing two kinds of biological macromolecules. In the first step, a short DNA sequence was used to produce an aqueous dispersion of SWCNTs. Afterwards, three plant viruses were investigated as protein shell donors. Therefore, we employed virus particles that exhibit different geometries and mechanical properties: the rigid rod-like TMV, the more flexible filamentous PVX, and the spherical CCMV.

The two filamentous virus candidates, TMV and PVX, did not show formation of hybrids with morphology corresponding to the original material. Although we observed a reassembly of these viruses' coat proteins upon exposure to CNTs, the VLP formation and the CNT coverage were incomplete. The rigid TMV tubes remained largely intact in SWCNT solution, however they were found to aggregate to the CNTs surface. The PVX virions formed inhomogeneous assemblies with DNA-dispersed CNTs. Thus, the presence of SWCNTs compromised the integrity of assembled viral tubes and therefore might also influence the infectivity of wild type virions. However further studies are required to confirm this.

In contrast, CCMV CPs were found to efficiently encapsulate DNA-dispersed SWNTs in virus-like particles. The viral coat proteins readily recognized the nucleic acid strands bound to the surface of SWCNTs as a suitable template and assembled around it in a helical way. The formed tubular structures were uniform in diameter and exhibited length corresponding to the dimension of the CNTs present in the solution. The random nucleation process and start of encapsidation were successfully imaged by TEM.

Surprisingly, the rod-like geometry of TMV and PVX showed no advantage in regard to assembly over the spherical CCMV in the performed experiments. One explanation for the poor encapsulation efficiency by the filamentous viruses could be the limited internal cavity size, which might be too small to accommodate CNTs dispersed with DNA. The cavity size of CCMV is approximately three times larger than inner cavity of TMV and PVX.

In conclusion, the presented encapsulation of SWCNT with CCMV CPs provides a new technique for highly homogenous surface functionalization of this carbon nanomaterial. This might greatly

promote new applications, for example in the field of biosensing and detection. The designed structure can be readily exploited when incorporating them in single nanotube devices and equipping the capsid protein with a receptor moiety[39-41].

2.4 Materials and methods

All chemicals were purchased from commercial sources (Sigma Aldrich, Acros Organics) and used as received without further purification. The DNA oligomer (5'-CCT CGC TCT GCT AAT CCT GTT A-3') was obtained from Biomers (Ulm, Germany) at HPLC purity grade. Copper grids (400 mesh) and holey carbon grids (Quantifoil 3.5/1) were purchased from Science Services (Germany). The sonication bath (VWR, The Netherlands, 150 W) was operated at 45 kHz. Centrifugal dialysis devices (Vivaspin 20, Sartorius Stedim) and dialysis membranes (RC, 6 Spectra/Por, Spectrum® Laboratories) were obtained from VWR. In all experiments, ultrapure water with a resistivity of 18.2 MΩ/cm was used. Absorption spectra were recorded on a UV-Vis spectrophotometer (Jasco V-630).

CCMV CP was provided by Prof. Dr. J.J.L.M. Cornelissen (MESA+ Institute, University of Twente, Enschede, The Netherlands).

TMV CP and PVX were provided by Dr. U. Commandeur (Institute of Biology, RWTH Aachen University, Aachen, Germany). TMV CP used in the experiments was equipped with His_6 and purified as a free CP from bacterial culture.

Dispersion and purification of SWCNT

The SWNT dispersion was prepared according to protocols reported elsewhere with slight modifications[19,42]. In short, a sample of HiPCO SWCNT (Carbon Nanotechnologies) was weighted into a 1.5 mL glass vial and placed in the ice-cold sonication batch. A dispersing buffer (1 mg/mL DNA, 0.1 M NaCl) to a total volume of 100 µL/100 µg of SWCNTs was added in 5 equal portions every 30 min. Dispersed SWCNTs were centrifuged for 1 hour at 60k rpm (Beckman Optima Ultracentrifuge) to remove insoluble material. Afterwards the supernatant was removed and washed once with 0.1 M NaCl solution in a centrifugal device with MWCO 10k to remove excess DNA. To the insoluble carbon material 1 mL of water was added and afterwards another centrifugation step was performed. The washed insoluble material was weighed to estimate

efficiency of dispersion. The final concentration of SWCNT in the solution was 80 μg/mL.

Coating with TMV capsid protein
TMV CP at a concentration of 400 μg/mL in 100 mM sodium acetate buffer pH=5.0, was mixed with SWCNT dispersion (6 μg/mL in 0.1 M NaCl) in 1:1 (v/v) ratio (1:66 weight ratio). Afterwards, the sample was incubated at RT for 2 hours. To visualize TMV CP re-assembly, TMV and SWCNT were mixed in 1:10 (v/v) ratio (1:6 weight ratio) and the incubation time was prolonged to 4 hours.

Coating with PVX capsid protein
The solution of PVX (400 μg/mL in 10 mM Tris HCl buffer pH=7.2) was mixed with SWCNTs dispersion (10 μg/mL in 0.1 M NaCl) in 1:1 (v/v) ratio and incubated overnight at 4°C. Prior to imaging the sample was diluted tenfold with ultrapure water.

Coating with CCMV capsid protein
First, the virus capsid solution was dialyzed overnight against a buffer solution containing 300 mM NaCl, 50 mM Tris, 1mM EDTA, 10mM $MgCl_2$, pH=7.4. Afterwards, the exact protein concentration (typically around 3.3 mg/mL) was determined by measuring absorption at 280 nm (ε=24.075 $M^{-1}cm^{-1}$). The concentration of SWCNT was adjusted to 6 μg/mL using 0.1 M NaCl and mixed with CP solution in 1:50 ratio (w/w). For full coverage the solution was incubated overnight at 4°C. To image early stage of VPL formation sample, the specimen was prepared after 1 minute of incubation at RT. In the control experiment, the DNA solution (1 mg/mL in 0.1 M NaCl) was mixed with CCMV CP solution in a 1:10 ratio (w/w) and incubated overnight at 4°C.

Transmission Electron Microscopy
The TEM samples were prepared by depositing 5 μL of sample on a glow-discharged carbon-coated copper grid (400 mesh). After 10 seconds, the excess of liquid was blotted on a paper filter. The sample was washed once with ultrapure water to remove salts. Then the samples were negatively stained with 2% uranyl acetate by depositing 5 μL of the stain solution for 10 seconds and blotting the excess on a paper filter (repeated twice). Pictures were collected on a Philips CM120 transmission electron microscope operated at 120kV in bright field mode.

Cryo Electron Microscopy

A drop of sample (2.7 µL) was deposited on a glow-discharged holey carbon-coated grid. Excess of solution was blotted off on a filter paper. The grid was subsequently vitrified in liquid ethane using a Vitrobot (FEI) and stored in liquid nitrogen before being transferred to a Philips CM 120 electron microscope equipped with a Gatan model 626 cryo-stage, operating at 120 kV. Images were taken in low-dose mode using a slow-scan CCD camera.

2.5 References

1. Davis, J.J.*, et al.* The immobilisation of proteins in carbon nanotubes. *Inorg Chim Acta* **272**, 261-266 (1998).
2. Kang, Y.*, et al.* On the spontaneous encapsulation of proteins in carbon nanotubes. *Biomaterials* **30**, 2807-2815 (2009).
3. Marchesan, S. & Prato, M. Under the lens: carbon nanotube and protein interaction at the nanoscale. *Chem Comm* **51**, 4347-4359 (2015).
4. Calvaresi, M. & Zerbetto, F. The Devil and Holy Water: Protein and Carbon Nanotube Hybrids. *Acc Chem Res* **46**, 2454-2463 (2013).
5. Dieckmann, G.R.*, et al.* Controlled assembly of carbon nanotubes by designed amphiphilic Peptide helices. *J Am Chem Soc* **125**, 1770-1777 (2003).
6. Grigoryan, G.*, et al.* Computational design of virus-like protein assemblies on carbon nanotube surfaces. *Science* **332**, 1071-1076 (2011).
7. Asuri, P.*, et al.* Increasing protein stability through control of the nanoscale environment. *Langmuir* **22**, 5833-5836 (2006).
8. Karajanagi, S.S., Vertegel, A.A., Kane, R.S. & Dordick, J.S. Structure and function of enzymes adsorbed onto single-walled carbon nanotubes. *Langmuir* **20**, 11594-11599 (2004).
9. Marchesan, S., Melchionna, M. & Prato, M. Carbon Nanostructures for Nanomedicine: Opportunities and Challenges. *Fuller Nanotub Car N* **22**, 190-195 (2014).
10. Harrison, B.S. & Atala, A. Carbon nanotube applications for tissue engineering. *Biomaterials* **28**, 344-353 (2007).
11. Fabbro, A., Bosi, S., Ballerini, L. & Prato, M. Carbon Nanotubes: Artificial Nanomaterials to Engineer Single Neurons and Neuronal Networks. *ACS Chem Neurosci* **3**, 611-618 (2012).
12. Vardharajula, S.*, et al.* Functionalized carbon nanotubes: biomedical applications. *Int J Nanomedicine* **7**, 5361-5374 (2012).
13. Rodriguez-Fernandez, L., Valiente, R., Gonzalez, J., Villegas, J.C. & Fanarraga, M.L. Multiwalled carbon nanotubes display microtubule

biomimetic properties in vivo, enhancing microtubule assembly and stabilization. *ACS Nano* **6**, 6614-6625 (2012).
14. Parra, J., Abad-Somovilla, A., Mercader, J.V., Taton, T.A. & Abad-Fuentes, A. Carbon nanotube-protein carriers enhance size-dependent self-adjuvant antibody response to haptens. *J Controll Rel* **170**, 242-251 (2013).
15. Holt, B.D.*, et al.* Carbon nanotubes reorganize actin structures in cells and ex vivo. *ACS Nano* **4**, 4872-4878 (2010).
16. Ge, C.*, et al.* Binding of blood proteins to carbon nanotubes reduces cytotoxicity. *Proc Natl Acad Sci U S A* **108**, 16968-16973 (2011).
17. Hazani, M.*, et al.* DNA-mediated self-assembly of carbon nanotube-based electronic devices. *Chem Phys Lett* **391**, 389-392 (2004).
18. Jung, S.*, et al.* Dissociation of single-strand DNA: single-walled carbon nanotube hybrids by Watson-Crick base-pairing. *J Am Chem Soc* **132**, 10964-10966 (2010).
19. Zheng, M.*, et al.* DNA-assisted dispersion and separation of carbon nanotubes. *Nat Mater* **2**, 338-342 (2003).
20. Kwak, M.*, et al.* Virus-like particles templated by DNA micelles: a general method for loading virus nanocarriers. *J Am Chem Soc* **132**, 7834-7835 (2010).
21. Kwak, M.*, et al.* DNA block copolymer doing it all: from selection to self-assembly of semiconducting carbon nanotubes. *Angew Chem Int Ed Engl* **50**, 3206-3210 (2011).
22. Yoon, H.*, et al.* Controlling exfoliation in order to minimize damage during dispersion of long SWCNTs for advanced composites. *Sci Rep* **4**, 3907 (2014).
23. Alonso, J.M., Gorzny, M.L. & Bittner, A.M. The physics of tobacco mosaic virus and virus-based devices in biotechnology. *Trends Biotechnol* **31**, 530-538 (2013).
24. van Rijn, P. & Boker, A. Bionanoparticles and hybrid materials: tailored structural properties, self-assembly, materials and developments in the field. *J Mat Chem* **21**, 16735-16747 (2011).
25. Klug, A. The tobacco mosaic virus particle: structure and assembly. *Philos Trans R Soc Lond B Biol Sci* **354**, 531-535 (1999).
26. Parker, L., Kendall, A. & Stubbs, G. Surface features of potato virus X from fiber diffraction. *Virology* **300**, 291-295 (2002).
27. Varma, A., Gibbs, A.J., Woods, R.D. & Finch, J.T. Some observations on the structure of the filamentous particles of several plant viruses. *J Gen Virol* **2**, 107-114 (1968).
28. Lee, K.L., Uhde-Holzem, K., Fischer, R., Commandeur, U. & Steinmetz, N.F. Genetic Engineering and Chemical Conjugation of Potato Virus X. *Virus Hybrids as Nanomaterials: Methods and Protocols* (eds. Lin, B. & Ratna, B.) 3-21 (Humana Press, Totowa, NJ, 2014).

29. Lico, C., Benvenuto, E. & Baschieri, S. The two-faced Potato Virus X: from plant pathogen to smart nanoparticle. *Frontiers in Plant Science* **6**(2015).
30. Scholthof, H.B., Scholthof, K.B. & Jackson, A.O. Plant virus gene vectors for transient expression of foreign proteins in plants. *Annu Rev Phytopathol* **34**, 299-323 (1996).
31. Marusic, C.*, et al.* Chimeric plant virus particles as immunogens for inducing murine and human immune responses against human immunodeficiency virus type 1. *J Virol* **75**, 8434-8439 (2001).
32. van Rijn, P.*, et al.* Morphology: Virus-SiO2 and Virus-SiO2-Au Hybrid Particles with Tunable Morphology *Part Part Syst Charact* **32**, 2-2 (2015).
33. Atabekov, J., Dobrov, E., Karpova, O. & Rodionova, N. Potato virus X: structure, disassembly and reconstitution. *Mol Plant Pathol* **8**, 667-675 (2007).
34. Nemykh, M.A.*, et al.* Comparative study of structural stabylity of potato virus X coat protein molecules in solution and in the virus particles. *Mol Biol (Mosk)* **41**, 697-705 (2007).
35. Goodman, R.M. Reconstitution of potato virus X in vitro. I. Properties of the dissociated protein structural subunits. *Virology* **68**, 287-298 (1975).
36. Ali, A., Shafiekhani, M. & Olsen, J. Molecular characterization of the complete genomes of two new field isolates of Cowpea chlorotic mottle virus, and their phylogenetic analysis. *Virus Genes* **43**, 120-129 (2011).
37. Speir, J.A., Munshi, S., Wang, G., Baker, T.S. & Johnson, J.E. Structures of the native and swollen forms of cowpea chlorotic mottle virus determined by X-ray crystallography and cryo-electron microscopy. *Structure* **3**, 63-78 (1995).
38. Mukherjee, S., Pfeifer, C.M., Johnson, J.M., Liu, J. & Zlotnick, A. Redirecting the coat protein of a spherical virus to assemble into tubular nanostructures. *J Am Chem Soc* **128**, 2538-2539 (2006).
39. Besteman, K., Lee, J.-O., Wiertz, F.G.M., Heering, H.A. & Dekker, C. Enzyme-Coated Carbon Nanotubes as Single-Molecule Biosensors. *Nano Lett* **3**, 727-730 (2003).
40. Star, A., Gabriel, J.-C.P., Bradley, K. & Grüner, G. Electronic Detection of Specific Protein Binding Using Nanotube FET Devices. *Nano Lett* **3**, 459-463 (2003).
41. So, H.-M.*, et al.* Single-Walled Carbon Nanotube Biosensors Using Aptamers as Molecular Recognition Elements. *J Am Chem Soc* **127**, 11906-11907 (2005).
42. Zheng, M.*, et al.* Structure-based carbon nanotube sorting by sequence-dependent DNA assembly. *Science* **302**, 1545-1548 (2003).